Asia-Pac. J. Atmos. Sci., 54(1), 77-90, 2018
DOI:10.1007/s13143-017-0061-0

pISSN 1976-7633 / eISSN 1976-7951

Numerical Study of the Role of Microphysical Latent Heating and Surface Heat Fluxes in a Severe Precipitation Event in the Warm Sector over Southern China

Jin-Fang Yin[1], Dong-Hai Wang[1], Zhao-Ming Liang[1], Chong-Jian Liu[1], Guo-Qing Zhai[2], and Hong Wang[3]

[1]*State Key Laboratory of Severe Weather, Chinese Academy of Meteorological Sciences, Beijing, China*
[2]*Department of Earth Science, Zhejiang University, Hangzhou, China*
[3]*Guangzhou Institute of Tropical and Marine Meteorology, China Meteorological Administration, Guangzhou, China*

(Manuscript received 9 October 2016; accepted 30 May 2017)

Abstract: Simulations of the severe precipitation event that occurred in the warm sector over southern China on 08 May 2014 are conducted using the Advanced Weather Research and Forecasting (WRF-ARWv3.5.1) model to investigate the roles of microphysical latent heating and surface heat fluxes during the severe precipitation processes. At first, observations from surface rain gauges and ground-based weather radars are used to evaluate the model outputs. Results show that the spatial distribution of 24-h accumulated precipitation is well reproduced, and the temporal and spatial distributions of the simulated radar reflectivity agree well with the observations. Then, several sensitive simulations are performed with the identical model configurations, except for different options in microphysical latent heating and surface heat fluxes. From the results, one of the significant findings is that the latent heating from warm rain microphysical processes heats the atmosphere in the initial phase of the precipitation and thus convective systems start by self-triggering and self-organizing, despite the fact that the environmental conditions are not favorable to the occurrence of precipitation event at the initial phase. In the case of the severe precipitation event over the warm sector, both warm and ice microphysical processes are active with the ice microphysics processes activated almost two hours later. According to the sensitive results, there is a very weak precipitation without heavy rainfall belt when microphysical latent heating is turned off. In terms of this precipitation event, the warm microphysics processes play significant roles on precipitation intensity, while the ice microphysics processes have effects on the spatial distribution of precipitation. Both surface sensible and latent heating have effects on the precipitation intensity and spatial distribution. By comparison, the surface sensible heating has a strong influence on the spatial distribution of precipitation, and the surface latent heating has only a slight impact on the precipitation intensity. The results indicate that microphysical latent heating might be an important factor for severe precipitation forecast in the warm sector over southern China. Surface sensible heating can have considerable influence on the precipitation spatial distribution and should not be neglected in the case of weak large-scale conditions with abundant water vapor in the warm sector.

Key words: Severe precipitation event, warm sector, microphysical latent heating, surface heat fluxes

Corresponding Author: Jin-Fang Yin, State Key Laboratory of Severe Weather, Chinese Academy of Meteorological Sciences, Beijing 100081, China.
E-mail: yinjf@cma.gov.cn

1. Introduction

For decades, observations have illustrated that severe precipitation events occur frequently during the period from April to June (named as "the first-rainy season"), concentrating on southern China (Huang, 1986). Among those severe precipitation events, one category of them takes place inside the warm sector ahead of a front zone which is far away from a surface front toward the north or northwest. One of the main characteristics of the severe precipitation events is that the surface front and cold air have no direct effects on the development of precipitation and the rainfall areas are always located in the warm sector, rather than in the frontal zone. Therefore, the severe precipitation is referred to as warm-sector rains in the first-rainy season in southern China (Zhou et al., 2003).

The severe precipitation events occurring in the warm sector in the first-rainy season over southern China have caused heavy casualties and loss of property. Therefore, considerable effort has been devoted to investigating the mechanism of formation and development for the severe precipitation. Since 1977, four field experiments have been conducted to understand the severe precipitation during the first rainy season over southern China (Huang, 1986; Zhou et al., 2003; Zhang et al., 2011a; Luo et al., 2017). More recently, the WMO/WWRP Research and Development Project (RDP) named as Southern China Monsoon Rainfall Experiment (SCMREX) has been launched with one of the goals to further understand the development of severe precipitation in the warm sector and the associated dynamical and microphysical processes (Luo et al., 2017).

The severe precipitation events occurring in the warm sector over southern China have complicated dynamic and microphysical processes. Zhang et al. (2011b) suggested that the low-level warm advection may play a more direct role in the development of mesoscale-beta convective systems, and the southerly warm and moist current contributes a lot to the severe precipitation formation (Zhao et al., 2007). Chen et al. (2012) discussed the systems for the warm-sector severe precipitation formation in southern China and proposed that the features of the circulation under 500 hPa can be divided into three types of shear lines, low vortexes and shear of southerly

wind velocity. Generally speaking, most of the studies have been focused on the effects of dynamical forcing on the severe precipitation events, such as cold air, low-level jet, local topography, and convergence line in the boundary layer. However, it is troublesome to explain the formation mechanism of the heavy precipitation occurred in the warm sector on the basis of the theories of frontal lifting and potential instability (Cheng and Bao, 1990). So far, it is still difficult to predict accurately the severe precipitation according to the large-scale environmental conditions, and thus the severe precipitation events are often missed by the forecasters in operational prediction (e.g., Du and Xue, 1985; Chen et al., 2003; Guan and Zhang, 2009).

Although some studies noticed the importance of cloud microphysical processes within the warm and wet air, little attention has been paid to further investigating the effects of the microphysics and thermodynamics on the development of cloud and precipitation in warm sector over southern China. For instance, Wen et al. (2006) proposed that latent heating makes vertical motion stretch further high. Wang et al. (2002) also noticed that the cold cloud processes play important roles in the formation and development of severe convective precipitation in Southern China.

Previous studies show that the severe precipitation events in the warm sector have apparent differences in terms of the rainfall features and its formation environment in the frontal zone (e.g., Zhao et al., 2008; Zhang and Ni, 2009; Luo et al., 2013). The severe precipitation events in the warm sector may have different microphysical processes and different initiation and maintenance mechanisms from those at the front. Observations show that the rain rate in the warm sector is generally much larger than that at the front zone, which may be related to microphysical processes within the warm and wet air (Cheng and Bao, 1990). To the best of the author's knowledge, much effort has been devoted to the large-scale weather conditions and external forcing systems associated with the severe precipitation events, and there is little information available in the literature about the roles of microphysical diabatic heating and surface heat fluxes in the development of severe precipitation in the warm sector over southern China.

Previous studies proposed that cloud microphysics plays a significant role on precipitation (e.g., Li et al., 2007; Tao et al., 2012; Li et al., 2013b). An interesting phenomenon is that the simulation with ice phase processes covered produces less rain over southern China than that of ice-free runs (Gao et al., 2006; Fu et al., 2011). This phenomenon somewhat contradicts the fact that ice phase processes are more effective than warm rain processes. This suggests that there are still some unknown mechanisms of the heavy rainfall initiation, development, and maintenance to be revealed for the warm sector. As early as in 1880s, Hazen (1889) noticed the importance of latent heating to precipitation. Liu and Moncrieff (2007) pointed out that latent heating profiles are largely comparable among the microphysical schemes, and surface precipitation is insensitive to the choice of cloud microphysics schemes. The aim of this study is to understand the cloud microphysical processes inside the warm sector region, and investigate the roles of microphysical latent heating as well as surface latent and sensible fluxes in the development of cloud and precipitation.

Following this introduction, Section 2 introduces the overview of the data and the severe precipitation event. A description of model configurations and simulation verifications is presented in Sections 3. An analysis of cloud microphysical properties is presented in Sections 4. The roles of warm rain and ice microphysics in the severe precipitation are given in Section 5. Results of sensitive experiments to surface latent and sensible heating are presented in Section 6. Section 7 gives a summary and discussion.

2. Data and case description

a. Datasets

The conventional observation data (including sounding and surface observations), ground-based weather radar, and the National Centers for Environmental Prediction Final Operational Global Analysis (NCEP-FNL) data are employed in this study. The precipitation data are obtained from the hourly automatic weather stations, which contain more than 40,000 stations over China. For the radar data, seven individual radar observations around Guangzhou station are used to generate the composite radar reflectivity. Those radar observations include Guangzhou, Meizhou, Shantou, Shenzhen, Zhanjiang, Shaoguang, and Yangjiang stations (Fig. 1). The large-scale flow and moisture field in the vicinity of the severe precipitation are investigated using the NCEP-FNL data, which has a horizontal resolution of 1-degree by 1-degree in the time interval of 6 hours. Except for the large-scale analysis, the NCEP-FNL datasets on the surface and 26 pressure levels from 1000 hPa to 10 hPa are also used as initialization and boundary conditions for the model simulations.

b. Rainfall process

Figure 1 shows the observational 24-h accumulated rainfall from 0000 UTC 08 to 0000 UTC 09 May 2014 over southern China. There were more than 10 rain gauge stations with 24-h accumulated rainfall exceeding 100 mm and the maximum value was 180 mm occurred at Shanwei station marked with a red hollow circle in Fig. 1. The main rainfall belt was mostly along with the coastline of southern China. Particularly, the severe precipitation occurred in the warm sector, which was far from the cold frontal zone. From the conventional synoptic analysis, it was almost impossible to predict accurately the intensity and location because the large-scale synoptic conditions were not beneficial to form severe precipitation event over southern China at that time. Consequently, operational forecasts almost missed the severe precipitation with the precipitation amount underestimated.

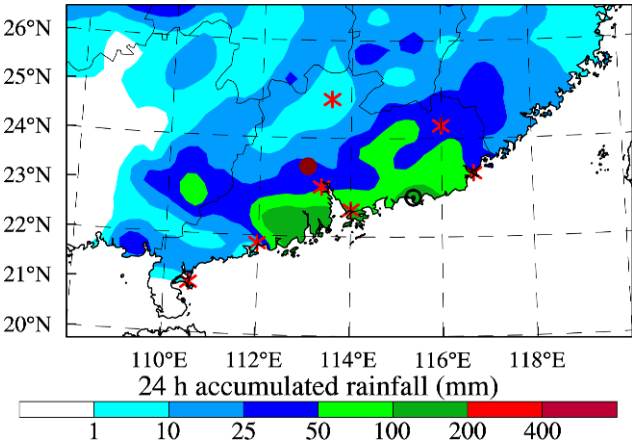

Fig. 1. Observational 24-h accumulated rainfall (mm) during the period from 0000 UTC 08 to 0000 UTC 09 May 2014. Black hollow circle is Shanwei station with the maximum rainfall of 180 mm; red dot is sounding station of Qingyuan; and asterisks are ground-based radar stations.

c. Large-scale conditions

The weather charts at 0000 UTC 08 May 2014 at 500 hPa and 700 hPa are presented in Fig. 2. At 500 hPa, the subtropical high (marked with 588 gpdm) was located over the western Pacific, which was far away from the coastline of southern China. There were two low-height centers over North China. One was located over northern China, and the other was located in north-western China. Both of the low-height centers were far away from southern China, and the surface front had no direct effects on the areas in the warm sector. Generally, the large-scale conditions were not favorable to the occurrence of precipitation over southern China. However, from Fig. 2b, the air was saturated at 700 hPa, and there was a strong southwesterly or southeasterly flow over Southern China. Previous studies (e.g., Zhao et al., 2007; Wu et al., 2010, 2011; Zhang et al., 2011b) indicate that the low-level flow with abundant water vapor is significant for severe precipitation to form over southern China.

Observation of the upper-air profile at 0000 UTC 08 May 2014 at Qingyuan station marked with a red dot in Fig. 1 over southern China is illustrated in Fig. 3. It is apparent that there was an extremely small (20 J kg^{-1}) convective available potential energy (CAPE) at this time. Generally, CAPE is a good indicator of the formation and development of convection and a favorable value of 1000 J kg^{-1} is usually necessary for convection development over southern China (e.g., Zhang et al., 2011b). Therefore, it is impossible to predict the severe precipitation event based on such a low CAPE and also on such a large CIN. It is worth noting that CAPE is very sensitive to temperature and humidity, and small variation of temperature or humidity can cause large change of CAPE (Bluestein and Jain, 1985). Besides, the lifting condensation level was 1005 hPa, with a temperature of 20°C. However, there was a large precipitable water of 40 mm, which might be a key factor of

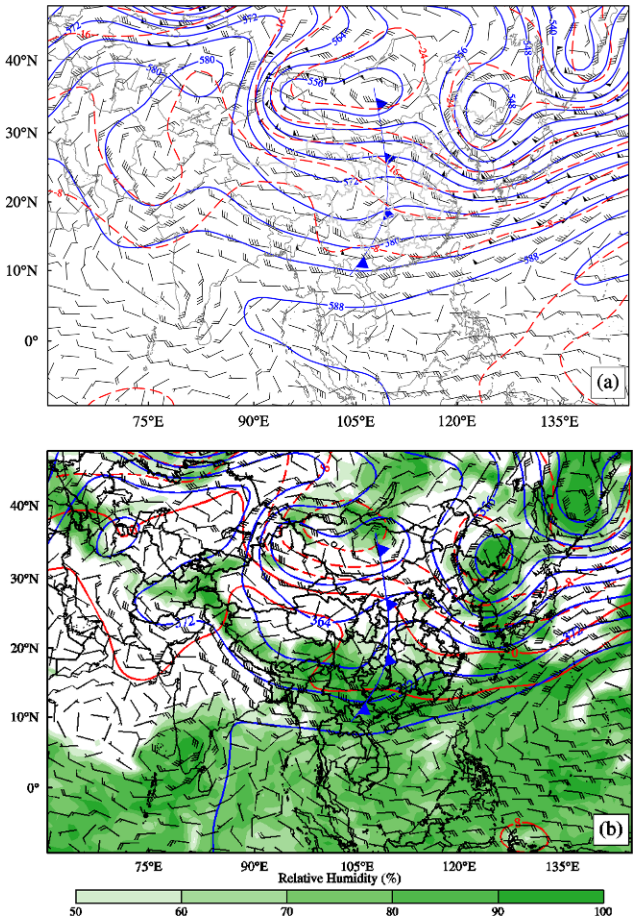

Fig. 2. Weather charts at 0000 UTC 08 May 2014 at (a) 500 hPa and (b) 700 hPa. Blue lines are geopotential height (units: gpdm), red lines represent temperature (°C), vectors indicate wind velocity (m s^{-1}), and the green shaded is relative humidity (%). The blue line with triangles is the cold front at surface.

the severe precipitation event. The profiles of dew-point temperature and temperature were overlapped below 700 hPa, implying that the air was saturated at those levels. In addition, southern China was characterized by southwesterly or southeasterly flows within the lower troposphere, and westerly flows were dominated at levels between 850 and 250 hPa.

3. Model configuration and simulation analyses

a. Model setup

The WRF-ARW (v3.5.1) model was set in a triple nested configuration at 36, 12, and 4 km, using one-degree NCEP-FNL dataset at intervals of six hours as the initialization and boundary conditions. The geographical coverage of each domain is shown in Fig. 4. According to the theory of Lindzen and Fox-Rabinovitz (1989), vertical resolution should be proportional to the horizontal resolution. Consequently, 57 sigma levels were used in the vertical and the model top was set to 20 hPa. Aligo et al. (2009) pointed out that precipitation is

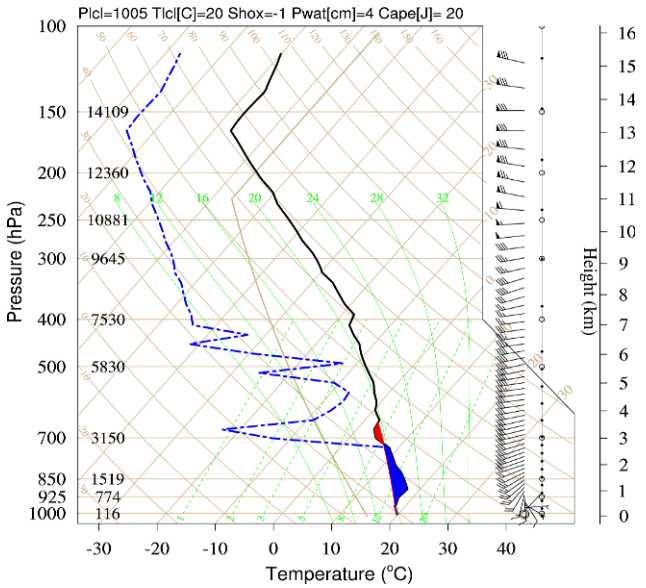

Fig. 3. Upper-air sounding data at 0000 UTC 08 May 2014 at Qingyuan station (marked with a red dot in Fig. 1) over southern China. The blue dot-dashed and thick black lines represent dew-point temperature and temperature, respectively. The shaded with red and blue colors are convective available potential energy (CAPE) and convective inhibition (CIN), respectively.

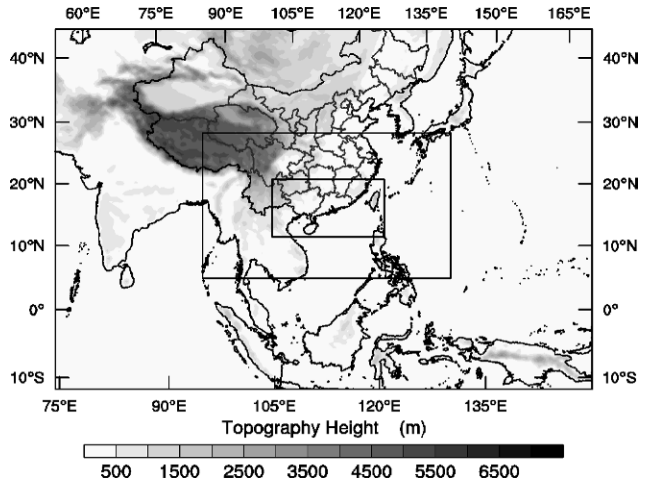

Fig. 4. Nested model domains used for the simulation of the severe precipitation event. The domain resolutions are 36 km, 12 km and 4 km, respectively. The shaded areas with gray color represent land.

sensitive to vertical grid resolution above the melting level and the surface layer. Therefore, the distribution of vertical levels was assigned to 15 levels below 850 hPa and 9 levels above 200 hPa, and the remaining levels were placed between 850 hPa and 200 hPa. The Kain-Fritsch (new Eta) cumulus parameterization scheme (Kain, 2004) was used for the outer two domains, and the scheme was turned off in the innest domain. The microphysical scheme was Yin scheme which is a newly developed double moment scheme based on long-term observations over East Asia (Yin, 2011, 2012, 2013, 2013a, 2014, 2005). The scheme predicts both the mixing ratios and particle number concentrations for six hydrometer species of cloud droplet, cloud ice, snow, rain, graupel, and hail, and the hydrometeor size distributions are represented by gamma functions. As for the shortwave and longwave radiative flux calculations, the rapid radiative transfer model scheme (Mlawer et al., 1997) was used. The Yonsei University (YSU) scheme (Hong et al., 2006) was introduced for the boundary layer, and the MM5 Monin-Obukhov scheme (Beljaars, 1995) was employed for the surface layer. The land surface model was Noah-MP scheme (Niu et al., 2011). The WRF model was run 24 hours starting at 0000 UTC 08 May 2014, with outputs at an interval of every hour, and it worked in non-hydrostatic mode and in two-way configuration with feedbacks.

b. Design of sensitive experiments

Previous studies (e.g., Wang et al., 2002; Wen et al., 2006) have proposed that latent heating made from cloud microphysical processes lead to vertical motion stretching high, which has significant impacts on the intensity of precipitation. In this study, a simulation with microphysical latent heating as well as surface sensible and latent heating was launched at first as control run (CTRL). Then, two categories of sensitive experiments were launched in order to investigate the effects of microphysical latent heating or surface sensible and latent heating on the precipitation. One category was characterized by turning off cloud microphysical latent heating, and the other with the surface sensible and latent heating turned off. It is worth noting that only the heating from microphysics was turned off for the former. It means that the temperature tendency was zeroed out (equivalent to no latent heat). However, other microphysical processes were not affected. In order to further illustrate the roles of warm rain microphysics and ice microphysics in the development of the severe precipitation, two sensitive simulations with either warm rain microphysics or ice microphysics only were performed. In the ice microphysics only experiment, the warm rain processes were not included. Therefore, the warm rain processes (e.g., condensation, auto-conversion from cloud water to rain water, the collision-coalescence cloud droplet by raindrop, etc.) were not activated. As a result, supersaturation was not considered when temp is warmer than 0°C. The interconversion between water vapor and ice hydrometeors would occur at a temperature below 0°C and rain water and cloud water were from ice particles melting at a temperature above 0°C. Note that the warm rain processes were not included in the ice microphysics only experiment, and vice versa. For the latter, both the surface sensible heating and latent heating were turned off first, and then the effects of the surface sensible heating or the latent heating were further tested separately. It should be noted that all the experiments were launched with identical physics options, initial and boundary conditions.

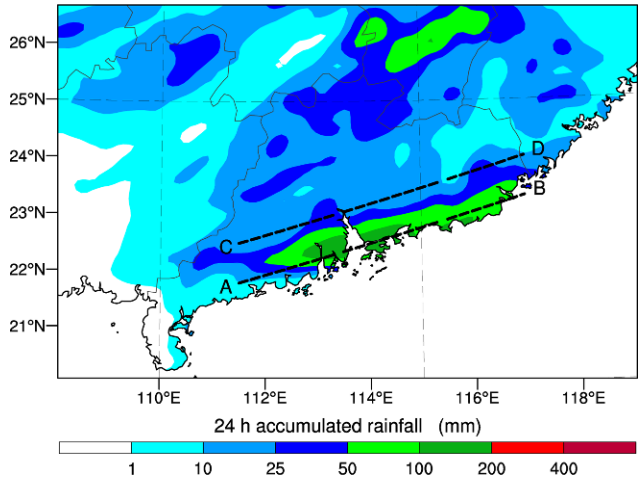

Fig. 5. Simulated 24-h accumulated precipitation (mm) during the period from 0000 08 UTC to 0000 UTC 09 May 2014. The dashed lines marked with A-B and C-D will be used for drawing profiles in next part.

c. Simulation verification

According to the simulation, both the domains of the horizontal resolution of 12 km and 4 km are able to reproduce the spatial distribution and evolution of the severe precipitation. From the model configuration, the cumulus parameterization is turned on in the 12 km domain, while the cumulus parameterization is not used in the 4 km domain. Cumulus parameterization has important effects of on severe precipitation in subtropical zone. Therefore, the 12 km results were chosen for all analysis in the next sections so as to keep the effects of cumulus parameterization on the precipitation. It should be noted that we focus the effects of cloud microphysics on the severe precipitation event in this work, while the effect of cumulus scheme was not investigated.

Simulation of 24-h (between 0000 UTC 08 to 0000 UTC 09 May 2014) accumulated rainfall amount is shown in Fig. 5. Compared to the observation (Fig. 1), the spatial distribution of the severe precipitation is well reproduced by the WRF model. It is obvious that the simulated severe precipitation belt along the coastline shows a good agreement with the observation. In addition, the model yields a peak value of 204 mm, which is close to the maximum observation value of 180 mm. However, the precipitation is a slightly overestimated over the regions to the north of 25°N. Moreover, the location of model's peak precipitation has a displacement to the observational station of Shanwei (marked with a red hollow circle in Fig. 1).

Figure 6 shows the composite radar reflectivity (CR) of both observation and simulation at 0600 and 1200 UTC, respectively. There are three CR belts at 0600 UTC. One is located over southern China from southwest toward to northeast, the second

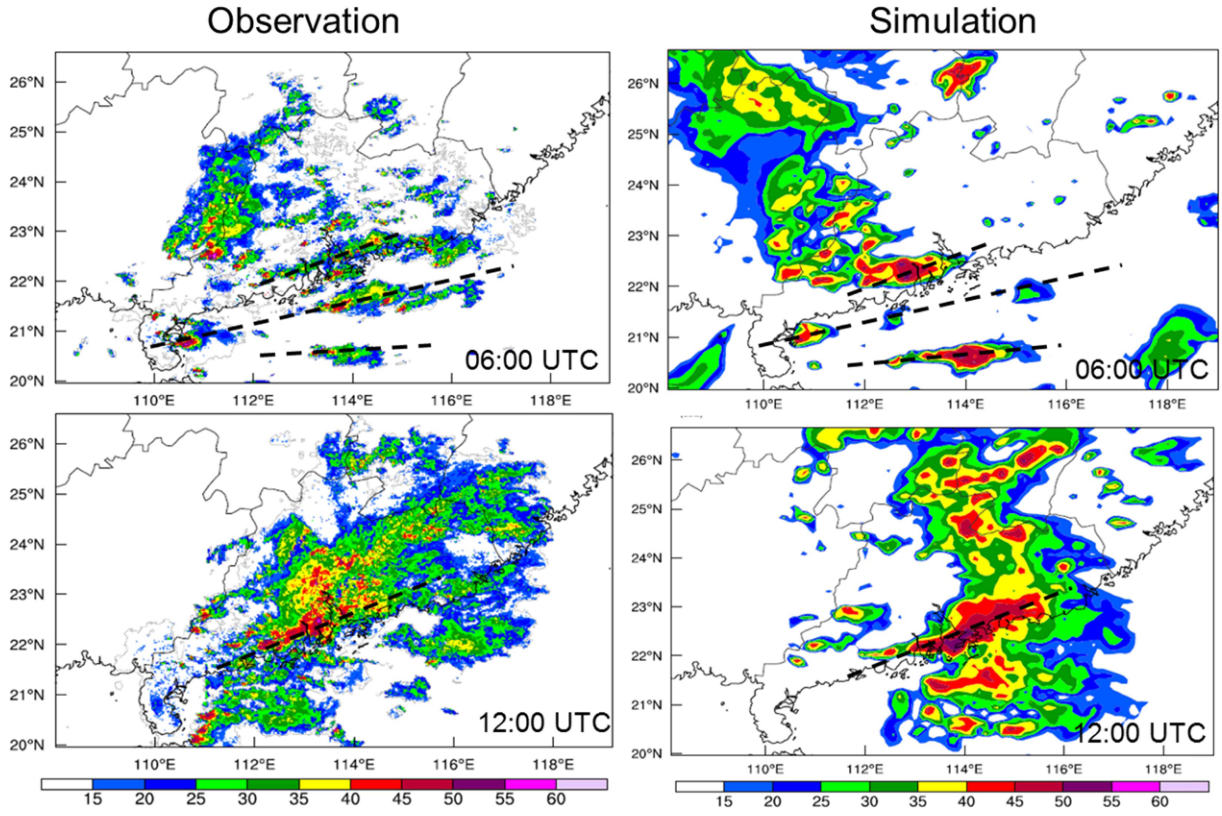

Fig. 6. Horizontal maps of simulation and observation composite radar reflectivity (dBz) at 0600 and 1200 UTC. The main radar reflectivity belts are marked with the black dashed lines.

one is near the coastline with three cells, and the third one is over the sea from west toward to east, which is far away from the coastline. At 1200 UTC, the strong CR is along the coastline from the southwest toward to northeast. It is apparent that the temporal and spatial distributions of the simulation agree well with the observations. To sum up, the WRF model is capable of simulating the major convective system development and reproduces the total surface rainfall amount as compared with the observations from the rain gauges and ground-based weather radars.

4. Cloud microphysical processes

a. Properties of hydrometeors

The distribution of cloud hydrometeor is one of the important properties of the microstructure of clouds. The evolution of the cloud hydrometeor reflects the dynamic and thermodynamic characteristics of a cloud system. Figure 7 shows the time-height cross sections of the averaged mixing ratios of water vapor, liquid (cloud (q_c) and rain (q_r)) and solid (cloud ice (q_i), snow (q_s), graupel (q_g), and hail (q_h)) hydrometeors from the 12 km spacing grid simulation. It is obvious that there is an abundant water vapor throughout the rainfall process. The water vapor decreases with the increasing height from surface to 8 km with the maximum value of water vapor greater than 16 g kg^{-1}. As for liquid hydrometeors, there are two layers with high values in the vertical distribution from 1000 to 1400 UTC. The lower one, which is mainly below 600 hPa, has a maximum value over 0.7 g kg^{-1}, and the upper one locates at the level between 300 and 500 hPa with a peak value of 0.45 g kg^{-1}. It should be noted that there is a large cloud water content concentrating on the levels between 500 and 300 hPa. This is because cloud droplets were transported by strong updraft in a short time. However, the cloud droplets did not freeze in such a short time (Xu et al., 2011). Rain water is mainly located below 600 hPa with the maximum rain mixing ratio of 0.7 g kg^{-1}, and the rain water enable to reach the ground.

Solid hydrometeors mainly appear above the height of 600 hPa with a peak value of 0.45 g kg^{-1} during the period of 1000-1400 UTC. Among the solid hydrometeors, graupel and cloud ice are major components. The results are consistent with the previous studies (e.g., McCumber et al., 1991; Krueger et al., 1995; Franklin et al., 2005), which proposed that graupel is the dominant frozen hydrometeor in the tropical and subtropical clouds due to abundant water vapor. Under this condition, cloud ice grows quickly forming a large number of graupel particles. On the contrary, there are low values of snow and hail mixing ratio in this simulation, which is similar to the results simulated with the Penn State/NCAR mesoscale model (MM5) given by Wen et al. (2006). In a few words, there are considerable cloud water, rain, cloud ice, graupel, while snow and hail are very small. Cloud ice and graupel occurs at the upper levels, and rain mainly concentrates at the lower levels. Cloud water had a widest spatial distribution, compared with

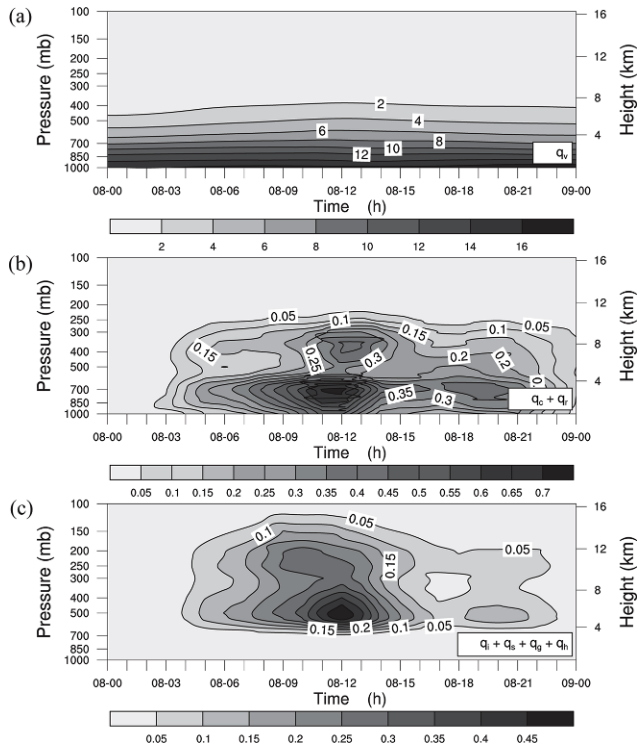

Fig. 7. Time -height cross sections of averaged mixing ratios of (a) water vapor, (b) liquid (q_c+q_r) and (c) solid (q_i+q_s+q_g+q_h) hydrometeors along line A-B in Fig. 5.

the other hydrometeors.

Compared the occurrence time of liquid hydrometeors and solid hydrometeors, the occurrence time of liquid hydrometeors is almost two hours earlier than that of solid hydrometeors. This indicates that warm rain microphysics processes are dominated processes in the initial stage, and then ice phase processes developed gradually, suggesting that the severe precipitation starts from warm rain microphysics processes. The results indicate that the latent heating from warm rain microphysics processes promotes convective systems to develop. The processes are similar to the ideal case with a temperature perturbation which is specified near the surface in the shape of a spherical bubble (called the “warm bubble”) for kicking off a convection. The latent heat from warm rain microphysical processes heated the atmosphere in the initial phase of the precipitation, and then the vertical motion started gradually. The upward motion further caused the release of latent heat. As a result, the vertical motion developed and the convective system formed by self-triggering and self-organizing. With the development of convection, ice phase processes are becoming more and more important for the severe precipitation formation. In other words, the severe precipitation event starts from the warm-rain process, and then cold-rain processes are activated. This is in line with the ideal model simulations given by Lou et al. (2003), which proposed that rain particles first come from auto-conversion of cloud droplets. Therefore, both warm rain and ice phase processes occur during the

period of precipitation, although the severe precipitation event occurs in the warm sector.

b. Effects of microphysical latent heating on precipitation

Observational and modeling studies have proposed that microphysical latent heating have important roles in precipitation development and dynamical processes (Magagi and Barros, 2004; Papritz and Pfahl, 2015; Pfahl et al., 2015). As stated above, the severe precipitation event occurs within the warm and moist air mass areas that are far away from cold fronts. Vertical profiles (marked with A-B and C-D in Fig. 5) of microphysical latent heating and vertical velocity at 0300 UTC 08 May 2014 are illustrated in Fig. 8. It is apparent from Fig. 8 that the microphysical latent heating is mainly located in the warm regions at a temperature above 0°C. The pattern of microphysical latent heating agrees well with the z-wind component. This indicates that the microphysical latent heating heats the atmosphere and thus triggers the development of vertical motion. One hour later, the vertical motion develops quickly and several convective systems forms gradually (figures not present here). The results are consistent with the ideal simulations given by Lin et al. (2005) who proposed that warm microphysics dominates the first 10 min, with accretion overshadowing auto-conversion as the first cell develops, in the warm season thunderstorms over the subtropical regions. Although there is no strong large-scale forcing system, the microphysical processes are able to form convective system by self-triggering and self-organizing.

Unlike to other studies (e.g., Tao et al., 2013; Li et al., 2013a), the effects of terrain are not important to the convective system development for the event. Li et al. (2013a) proposed that a local low terrain have strong effects on precipitation development and spatial distribution by changing boundary layer convergence and ascending motion. In this study, however, the profile marked with C-D indicates that there was also vertical motion around the terrain, but the convection was not developed. This suggests that topography is not important for the event, and the precipitation is intensified through the microphysical latent heating, rather than by dry topographic-flow dynamics. This is probably because there is very weak large- and meso-scale dynamical forcing over the warm sector.

Figure 9 shows the vertical profiles of 24-h averaged total liquid water content (q_r plus q_c) and ice water content (q_i, q_s, q_g, plus q_h) along line A-B and C-D in Fig. 5. Liquid water is mainly located at the temperature above 0°C, with the maximum value greater than 0.50 g kg^{-1}. Most of the ice water concentrates on the levels with temperature below 0°C and the ice water enable to reach a height near 15 km. There are two large value cores of ice water content. The lower one concentrates on the levels between 5 and 9 km with the maximum value of 0.50 g kg^{-1}, the other locates at the level between 10 and 13 km with the maximum value of 0.25 g kg^{-1}. The distribution patterns are in agreement with the results provided by Yin et al. (2013b) in which studies cloud vertical profiles over East Asia are investigated using the CloudSat datasets. It

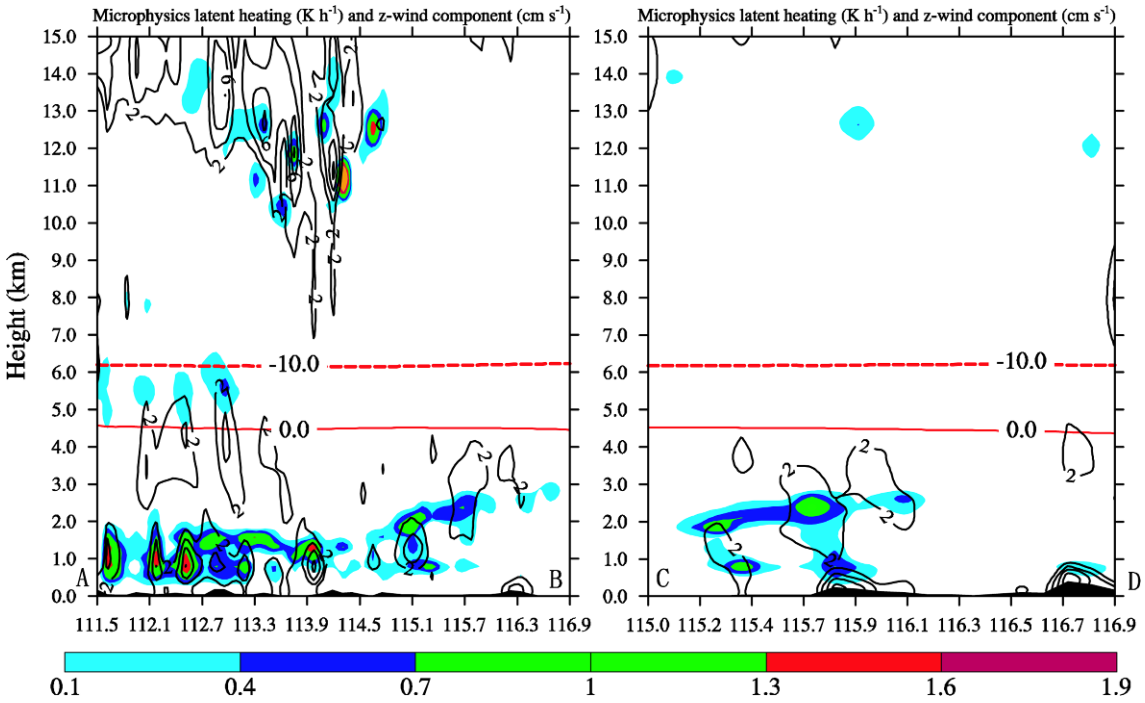

Fig. 8. Vertical profiles (marked with A-B and C-D in Fig. 5) of microphysical latent heating (shaded, K h^{-1}) and z-wind component (contour, cm s^{-1}) after the model integration of 3 hours. The red lines present the heights of temperature at −10.0°C (dashed) and 0°C (solid), and the shaded with black is terrain.

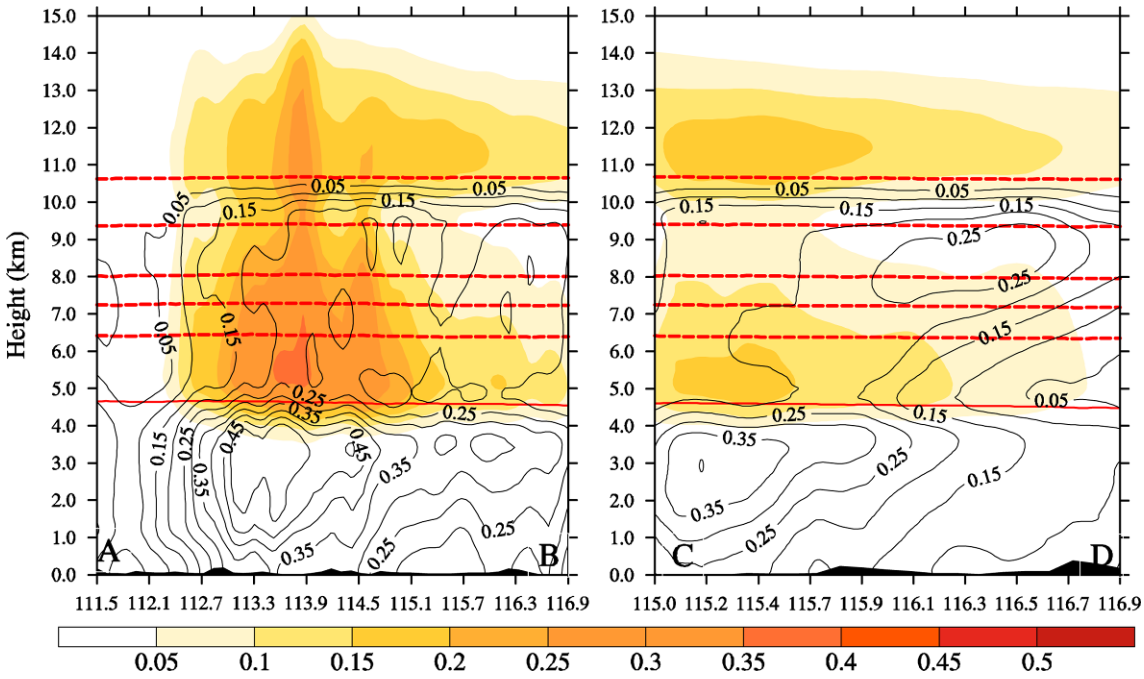

Fig. 9. Vertical profiles of 24-h averaged total liquid water content (rain water and cloud water, contour) and ice water content (cloud ice, snow, graupel and hail, shaded) along line A-B and C-D in Fig. 5. The red lines present the heights with temperatures at 0, −10, −15, −20, −30 and −40°C from bottom to up, and the shaded with black is terrain.

should be emphasized that the two ice water cores with large value formed from different microphysical processes. The upper one is formed by the homogeneous freezing of cloud droplets, where cloud water immediately freezes to form cloud ice when cloud temperature is less than 237.15 K or a cloud is located higher than 10 km (Yin et al., 2013b). However, the lower one is caused by ice nucleation, riming, accretion and collision-coalescence processes (Hobbs et al., 1974).

Obviously, distinct patterns can be found between A-B and C-D profiles. It is apparent that both the liquid water content and ice water content along line A-B is much larger than those along line C-D. Although the severe precipitation event occurs in the warm sector, the precipitation event has similar microphysical processes to a cool cloud precipitation. Previous studies such as Wen et al. (2006) suggested that a mixed ice phase microphysical scheme reproduced better precipitation than a warm scheme for a heavy rainfall over southern China. Wang et al. (2002) also noticed that the cold cloud process in which ice phase is coexisted with super-cooled liquid phase of cloud water plays the most important role in the formation and development of convective severe precipitation over southern China. It is well known that ice phase microphysical processes are more efficient to form large size drops than that of warm cloud processes (Fovell and Ogura, 1988; McCumber et al., 1991; Tao et al., 2003; Gao et al., 2006). Therefore, the ice phase microphysical processes contribute a lot to the severe precipitation formation. This phenomenon is also seen from the Fig. 5 in which there is a strong rainfall along line A-B, but a weak precipitation along line C-D.

5. Roles of warm rain and ice microphysics

Figure 10 presents the simulation of 24-h accumulated precipitation from the simulations with either warm rain microphysics or ice microphysics only. As for the simulation with warm rain microphysics only (Fig. 10a), there is a wide range of precipitation area with the maximum precipitation is greater than 100 mm, implying that severe precipitation can occur even without ice microphysical processes. However, the spatial distribution of precipitation is quite different to observation. Without the ice microphysics, there is no feedback of ice microphysics on the large-scale fields, and thus the effects of the large-scale fields on the precipitation spatial distribution are eliminated (Grabowski, 2003). Grabowski (2003) proposed that without ice microphysics would reduce stratiform component and short life cycle of mesoscale systems, which influences scale selection of the large-scale convectively-coupled gravity waves and the vertical transport of horizontal momentum. As a result, the precipitation spatial distribution is altered. If only the warm rain microphysics is used, the WRF model cannot capture the characteristics of the severe precipitation in warm sector, and thus the spatial distribution is modified.

Regarding the simulation with ice microphysics only (Fig. 10b), there is a very weak precipitation over southern China, while a large precipitation occurs in north region with the precipitation over 50 mm. The heavy precipitation might be related to the northern frontal synoptic systems. The strong rainfall belt along the coastline is completely missed. In the case without warm rain processes, the convective systems are

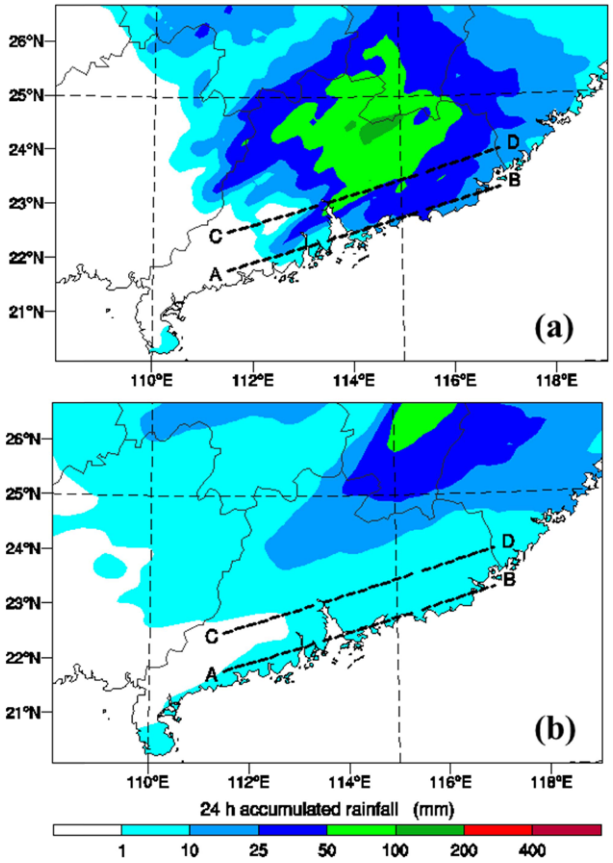

Fig. 10. As in Fig. 5 but with (a) only warm rain microphysics and (b) only ice microphysics covered.

unable to form, and thus the severe precipitation is not formed. This is because the latent heating from warm rain microphysics processes is eliminated, and thus strong vertical motion is not triggered. As a result, convective systems are not developed, and thus the precipitation is unable to form in the warm sector over southern China.

From the above, it is found that the warm rain processes play crucial roles in the development of precipitation in the warm sector, which promotes convective system development by self-triggering and self-organizing through latent heating from warm rain microphysics. Severe precipitation event can occur in the warm sector even without ice microphysical processes, but the spatial distribution of precipitation is altered. This may be related to the feedbacks of ice microphysics on large-scale fields (Grabowski, 2003; Wang et al., 2010). However, without warm rain processes, convective systems are not trigged and developed, and thus the precipitation cannot be formed in the warm sector.

6. Sensitivity to latent and sensible heating

a. Sensitivity to microphysical latent heating

Figure 11 shows the simulation of 24-h accumulated precipitation using the scheme without microphysics latent heating. It is apparent that the 24-h accumulated precipitation is less than 25 mm with several rainfall centers locating on the southern China. Compared to the simulations with microphysics latent heating turned on, it is found that there is a very weak precipitation, and the strong rainfall belt along the coastline is not reproduced at all. It can be concluded that the microphysics latent heating has significant contribution to forming severe precipitation in the warm sector over southern China. Without microphysics latent heating, convective systems are not organized, and thus the severe precipitation cannot be reproduced. The results are consistent with the effects of condensation heating on the precipitation of meso-scale convective system over southern China (Qian and Shen, 1990; Meng et al., 2005; Li et al., 2016).

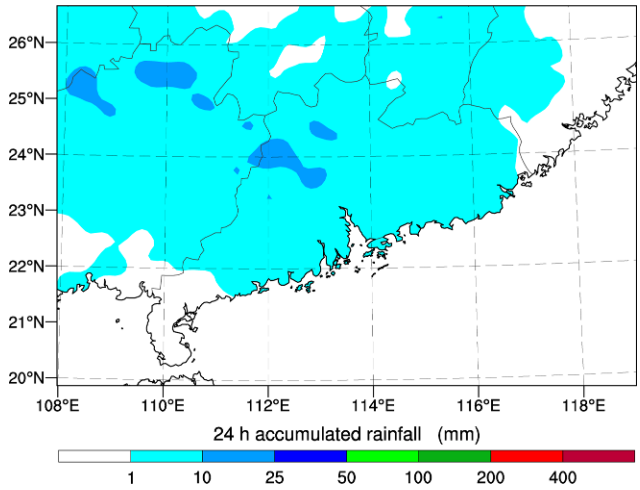

Fig. 11. As in Fig. 5 but without microphysics latent heating.

Figure 12 shows the vertical profiles of 24-h averaged total liquid water content and ice water content along line A-B and C-D marked in Fig. 5. Compared to CTRL (Fig. 10), there is a smaller liquid and ice water content when the microphysical latent heating is turned off. In addition, the liquid water content is mainly located at the low levels below 2 km. Without microphysical latent heating, there is no enough energy to promote the development of a convective system. As a result, there only is an extreme weak vertical motion (Fig. 13), and thus the severe precipitation fails to develop. Although the warm rain processes play dominant roles in the microphysical processes at the low levels, ice phase processes are not triggered largely under this condition. Consequently, only a small precipitation occurs from weak cloud microphysics processes. Note that there exists a large ice hydrometeor zone with temperature below −40°C. This happens because of the heterogeneous process of cloud droplets in low temperature condition (Baker, 2001). However, it does not have a contribution to forming large precipitation drops due to its location at higher levels.

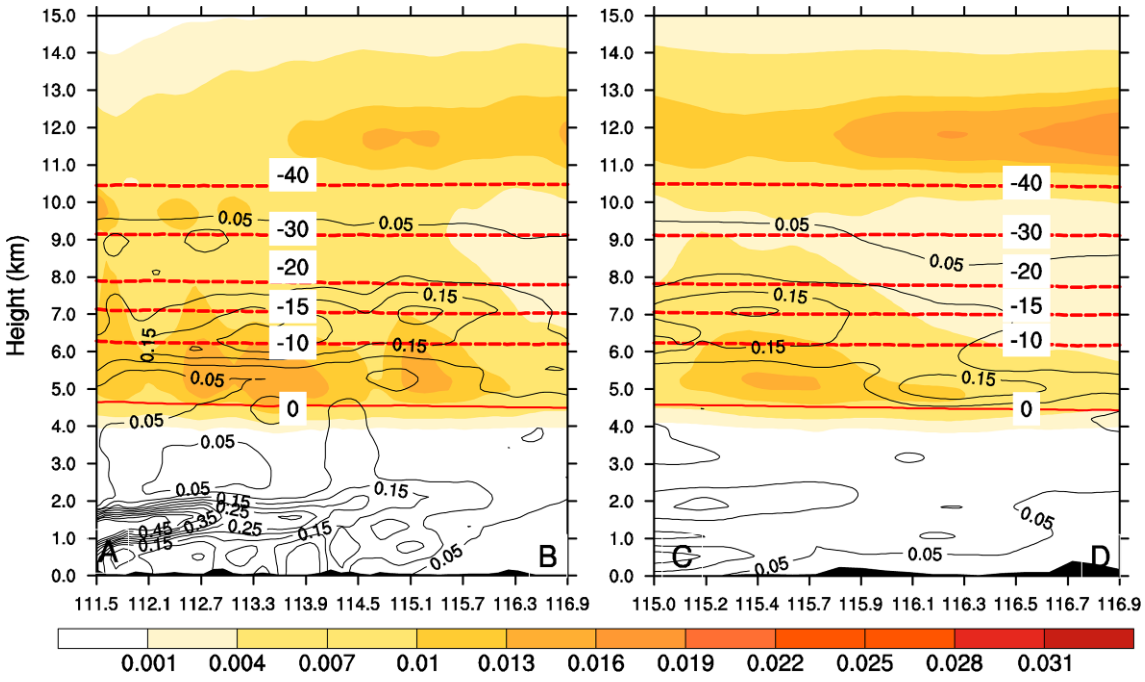

Fig. 12. As in Fig. 9 but without microphysics latent heating.

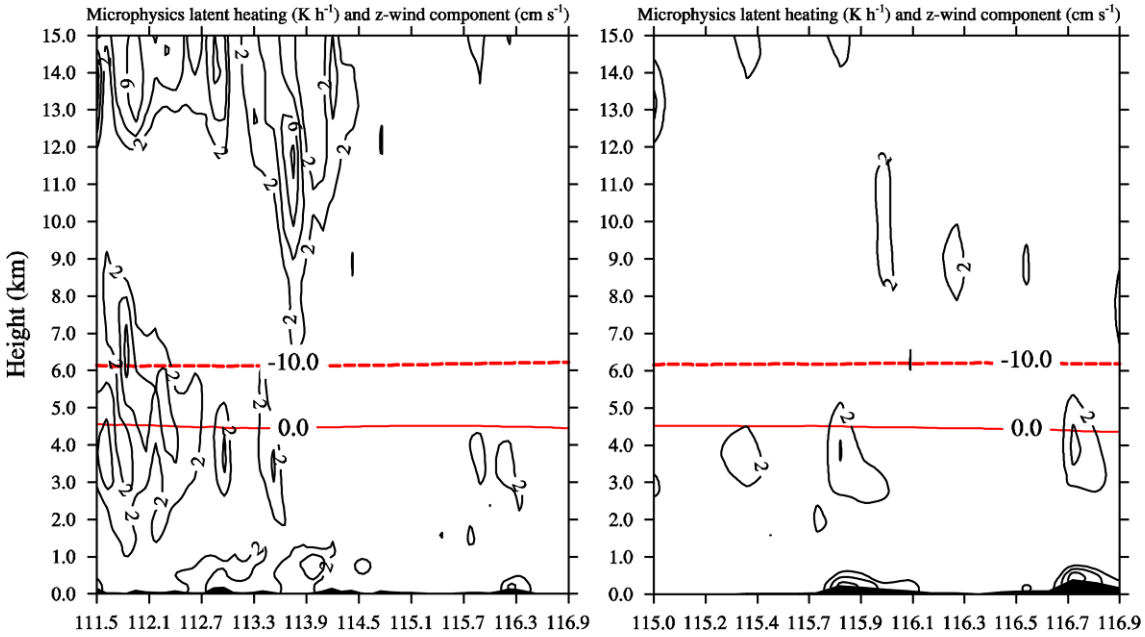

Fig. 13. Vertical profiles (marked with A-B and C-D in Fig. 5) of z-wind component (contour, cm s^{-1}) after the model integration of 3 hours. The red lines present the heights of temperature at −10.0°C (dashed) and 0°C (solid), and the shaded with black is terrain.

b. Sensitivity to surface heat fluxes

The simulation of 24-h accumulated precipitation (mm) without both surface sensible and latent heating is shown in Fig. 14. Compared to CTRL (Fig. 5), the precipitation spatial distribution is spread and the severe precipitation cores are altered. The severe precipitation belt along the coastline is weakened, while the areas of rainfall with an amount between 50 and 100 mm are significant extended northwestward. A severe precipitation core with an amount over 100 mm occurs in the central part. Generally speaking, the precipitation spatial distribution changes a lot with the range spread, when both the

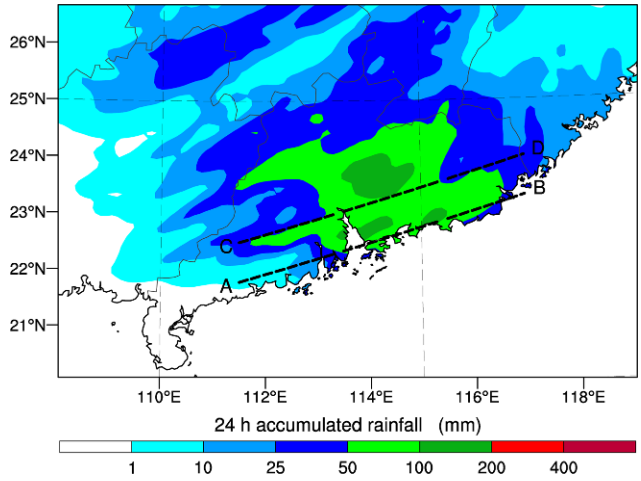

Fig. 14. As in Fig. 5 but without both surface sensible and latent heating.

surface sensible and latent heating are turned off. The results indicate that the surface sensible and latent heating has distinct influences on determining the spatial distribution and intensity of the precipitation. Note that the surface sensible and latent heating show a less influence on the severe precipitation, compared to the case of latent heating from cloud microphysics.

In order to investigate the effects of surface sensible and latent heating on precipitation, two more sensitive experiments were performed with surface sensible heating or latent heating turned off separately. Figure 15 shows 24-h accumulated precipitation that is simulated without surface sensible heating (Fig. 14a) or latent heating (Fig. 14b). Generally, the precipitation intensity is comparable to those of observation (Fig. 1) and the simulation with both surface sensible heating and latent heating turned on (Fig. 5). However, their effects on the precipitation spatial distribution are very different. In the case without surface sensible heating (Fig. 14a), the severe precipitation belt jumped northward about half a degree of latitude, implying that the surface sensible heating has strong effects on the spatial distribution, but small effects on the precipitation intensity. Lolis et al. (2004) put forward that sensible and latent heat fluxes contribute significantly to depression development, and the depressions form advect cold and dry air masses. Besides, the depressions lead to a southerly airflow with potential instability. Thielen et al. (2000) pointed out that increased surface sensible heat flux produces high-reaching convection, resulting in the development of rainwater and accumulated rainfall. By turning off surface sensible heating, the spatial distribution convective cores are altered, and thus the characteristics of convective systems and their precipitation are modified.

In the case without latent heating (Fig. 14b), the precipitation patterns are not altered dramatically. The spatial distribution and intensity of the total rainfall is close to those of observation (Fig. 1) and simulation (Fig. 5) with both surface

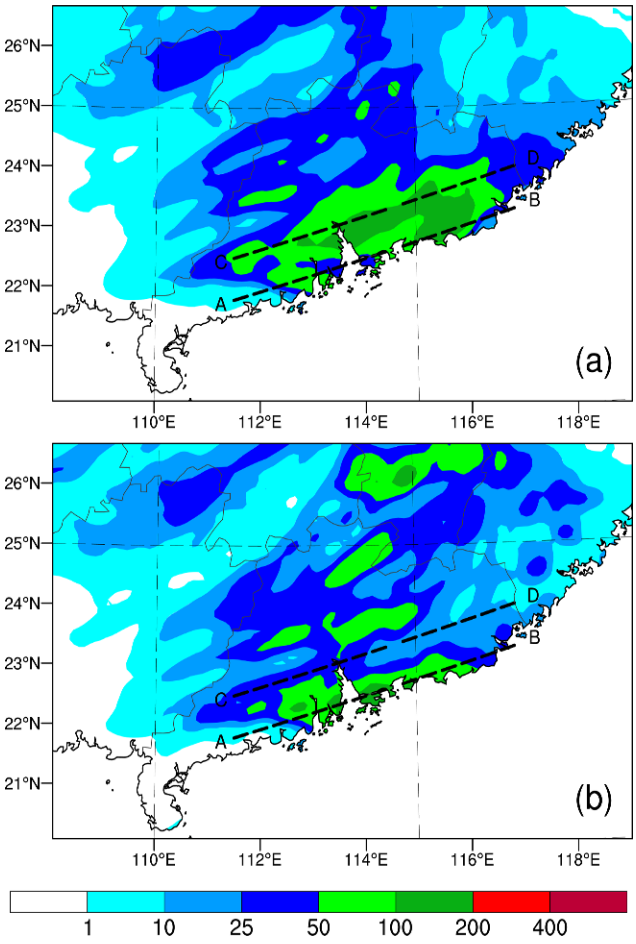

Fig. 15. As in Fig. 5 but without (a) surface sensible heating and (b) surface latent heating.

sensible heating and latent heating turned on. The strong rainfall belt along the coastline is still reproduced, although the range of rainfall over 100 mm is somewhat reduced. It is worth noting that two false rainfall belts are produced over southern China.

Generally, both the surface sensible and latent heating have effects on the rainfall spatial distribution and intensity. Comparatively speaking, surface sensible heating has more influence on the rainfall spatial distribution than that of surface latent heating. More specifically, the surface sensible heating has strong influences on the rainfall spatial distribution, while the surface latent heating has only a slightly impact on the rainfall intensity. It is highlighted that surface sensible heating can have considerable influence on the precipitation spatial distribution and should not be neglected in the case of weak large-scale conditions with abundant water vapor in the warm sector. It should be noted that the effect mechanism of the surface sensible and latent heating on precipitation was not fully explain in this study. We just investigated the importance of the microphysical latent heating and the surface heat fluxes. The results suggest that the surface heat fluxes have less

influence on the severe precipitation, compared to the case of latent heating from cloud microphysics.

7. Concluding remarks

In this study, the roles of microphysical latent heating and surface heat fluxes in the severe precipitation event that occurred on 8 May 2014 over southern China have been analyzed based on the numerical simulations by using the Advance Weather Research and Forecasting (WRF-ARW) model. The detailed conclusions are as follows.

(1) Warm rain microphysical processes at the low levels play key roles in the initial phase of the precipitation development. Latent heating from the warm rain processes heats the atmosphere, and thus starts the development of vertical motion in the initial phase and thus promote the formation of convective systems by self-triggering and self-organizing, although the environmental conditions are not favorable to the occurrence of precipitation event.

(2) Not only warm rain microphysical processes, but also ice phase microphysical processes are active during the period of the precipitation over the warm sector. However, the ice microphysics processes occurs almost two hours later than the warm rain microphysical processes. The warm rain processes promote the convective system development in the initial phase of the precipitation, and the ice phase microphysical processes have significant influences on the spatial distribution of the severe precipitation.

(3) The total rainfall in the warm sector is very sensitive to the latent heating of microphysics. When the latent heating of microphysics is turned off, deep convective system cannot be triggered, and thus there is a very weak precipitation without heavy rainfall belt occurrence.

(4) Both surface sensible and latent heating have effects on rainfall intensity and spatial distribution. Comparatively speaking, the surface sensible heating has strong influences on the rainfall spatial distribution, while the surface latent heating has only a slightly impact on rainfall intensity.

The roles of microphysical latent heating and surface heat fluxes in the severe precipitation have been investigated in this study. However, the triggers for the activation of microphysics latent heat have not been found. This might be associated with very microscale systems (such as turbulence, rotors in the boundary layer) due to low model resolution. Further studies will be continued by employing high resolution (e.g., large-eddy) simulations so as to provide well understanding of the trigger conditions in the future. Also, the upstream shortwave might play an important role in triggering the development of the heavy rainfall event. Besides, previous studies have confirmed that cloud processes and associated feedbacks have strong influences on meso- and large-scale atmospheric circulations (e.g., Tao and Simpson, 1993; Zängl, 2007; Kumar et al., 2013). Another interesting phenomenon of the severe precipitation in the warm sector over southern China is that the precipitation often occurs along the coastline of southern China (Chen et al., 2014). This might suggest that the interactions between land and ocean play an important role in the precipitation formation (Qian, 2008; Mechoso et al., 2013). Therefore, further studies are required to understand the roles of interactions between cloud microphysics, thermodynamics and dynamics in severe precipitations over the warm sector in the future.

Acknowledgements. This study is jointly supported by National Natural Science Foundation of China (No. 41405006), National Department Public Benefit Research Foundation (Nos. GYHY201406003 and GYHY201506002), and Basic Research Fund of the Chinese Academy of Meteorological Sciences (Nos. 2014R016 and 2015Z003). We thank the three anonymous reviewers for providing constructive comments and suggestions, which greatly improved the quality of the paper.

Edited by: John Richard Gyakum

References

Aligo, E. A., W. A. Gallus Jr., and M. Segal, 2009: On the impact of WRF model vertical grid resolution on midwest summer rainfall forecasts. *Wea. Forecasting*, **24**, 575-594.

Baker, M., 2001: Cloud physics: Inside history on droplets. *Nature*, **413**, 586-587.

Beljaars, A. C. M., 1995: The parameterization of surface fluxes in large-scale models under free convection. *Quart. J. Roy. Meteor. Soc.*, **121**, 255-270.

Bluestein, H. B., and M. H. Jain, 1985: Formation of mesoscale lines of pirecipitation: Severe squall lines in oklahoma during the spring. *J. Atmos. Sci.*, **42**, 1711-1732.

Chen, J., J. Xue, and H. Yan, 2003: The uncertainty of mesoscale numerical prediction of south China heavy rain and the ensemble simulations. *Acta Meteor. Sin.*, **61**, 432-446 (In Chinese with English abstract).

Chen, X.-X., Z. Ding, C. Liu, Y. Chang, and C. Zhu, 2012: Statistic analysis on the formation system of warm-sector heavy rainfall in may and june from 2000-2009. *J. Trop. Meteorol.,* **28**, 707-718 (in Chinese with English abstract).

Chen, X., K. Zhao, and M. Xue, 2014: Spatial and temporal characteristics of warm season convection over Pearl River Delta region, China, based on 3years of operational radar data. *J. Geophy. Res.*, **119**, 12447-12465, doi:10.1002/2014JD021965.

Cheng, Z., and C. Bao, 1990: Numerical simulation of heavy rain in a moist atmosphere. *Acta Meteor. Sin.*, **48**, 480-485 (in Chinese with English abstract).

Du, J., and H. Xue, 1985: An investigate of the intensity and location of a heavy rainfall in warm sector. *J. Trop. Meteorol.*, **1**, 85-92 (in Chinese).

Fovell, R. G., and Y. Ogura, 1988: Numerical simulation of a midlatitude squall line in two dimensions. *J. Atmos. Sci.*, **45**, 3846-3879.

Franklin, C. N., G. J. Holland, and P. T. May, 2005: Sensitivity of tropical cyclone rainbands to ice-phase microphysics. *Mon. Wea. Rev.*, **133**, 2473-2493.

Fu, D., X. Guo, and C. Liu, 2011: Effects of cloud microphysics on monsoon convective system and its formation environments over the South China Sea: A two-dimensional cloud-resolving modeling study. *J. Geophys. Res.*, **116**, D07108, doi:10.1029/2010JD014662.

Gao, S., L. Ran, and X. Li, 2006: Impacts of ice microphysics on rainfall and thermodynamic processes in the tropical deep convective regime: A

2D cloud-resolving modeling study. *Mon. Wea. Rev.*, **134**, 3015-3024.

Grabowski, W. W., 2003: Impact of ice microphysics on multiscale organization of tropical convection in two-dimensional cloud-resolving simulations. *Quart. J. Roy. Meteor. Soc.,* **129**, 67-81.

Guan, J., and L. Zhang, 2009: Application of the method of BGM in medium-range ensemble forecast for a south China rainstorm. *J. Trop. Meteorol.*, **25**, 246-250 (in Chinese with English abstract).

Hazen, H. A., 1889: Rainfall and latent heat. *Science*, **327**, 369-369.

Hobbs, P. V., S. Chang, and J. D. Locatelli, 1974: The dimensions and aggregation of ice crystals in natural clouds. *J. Geophys. Res.*, **79**, 2199-2206.

Hong, S.-Y., Y. Noh, and J. Dudhia, 2006: A new vertical diffusion package with an explicit treatment of entrainment processes. *Mon. Wea. Rev.*, **134**, 2318-2341.

Huang, S. S., 1986: *Heavy Rainfall over Southern China in the Pre-Rainy Season*. Guangdong Science and Technology Press, 244 pp (in Chinese).

Kain, J. S., 2004: The kain-fritsch convective parameterization: An update. *J. Appl. Meteorol.*, **43**, 170-181.

Krueger, S. K., Q. Fu, K. N. Liou, and H.-N. S. Chin, 1995: Improvements of an ice-phase microphysics parameterization for use in numerical simulations of tropical convection. *J. Appl. Meteorol.*, **34**, 281-287.

Kumar, S., A. Hazra, and B. N. Goswami, 2013: Role of interaction between dynamics, thermodynamics and cloud microphysics on summer monsoon precipitating clouds over the Myanmar Coast and the Western Ghats. *Climate Dyn*., **43**, 911-924, doi:10.1007/s00382-013-1909-3.

Li, B., L. P. Liu, S. X. Zhao, and C. Y. Huang, 2013a: Numerical experiment of the effect of local low terrain on heavy rainstorm of South China. *Plateau Meteor.*, **32**, 1638-1650, doi:10.7522/j.issn.1000-0534.2012.00156 (In Chinese with English abstract).

Li, J., G. Wang, W. Lin, Q. He, Y. Feng, and J. Mao, 2013b: Cloud-scale simulation study of Typhoon Hagupit (2008) Part II: Impact of cloud microphysical latent heat processes on typhoon intensity. *Atmos. Res.*, **120**, 202-215, doi:10.1016/j.atmosres.2012.08.018.

_____, K. Wu, F. Li, Y. Chwn, and Y. Huang, 2016: Cloud-scale simulation study on the evolution of latent heat processes of mesoscale convective system accompanying heavy rainfall: The Hainan case. *Atmos. Res.*, **169**, 331-339, doi:10.1016/j.atmosres.2015.10.014.

Li, Y., W. Huang, and J. Zhao, 2007: Roles of mesoscale terrain and latent heat release in typhoon precipitation: A numerical case study. *Adv. Atmos. Sci.*, **24**, 35-43.

Lin, H., P. K. Wang, and R. E. Schlesinger, 2005: Three-dimensional nonhydrostatic simulations of summer thunderstorms in the humid subtropics versus High Plains. *Atmos. Res.*, **78**, 103-145, doi:10.1016/j.atmosres.2005.03.005.

Lindzen, R. S., and M. Fox-Rabinovitz, 1989: Consistent vertical and horizontal resolution. *Mon. Wea. Rev.*, **117**, 2575-2583.

Liu, C., and M. W. Moncrieff, 2007: Sensitivity of cloud-resolving simulations of warm-season convection to cloud microphysics parameterizations. *Mon. Wea. Rev.*, **135**, 2854-2868.

Lolis, C. J., A. Bartzokas, and B. D. Katsoulis, 2004: Relation between sensible and latent heat fluxes in the Mediterranean and precipitation in the Greek area during winter. *Int. J. Climatol.*, **24**, 1803-1816.

Lou, X., Z. Hu, Y. Shi, P. Wang, and X. Zhou, 2003: Numerical simulations of a heavy rainfall case in South China. *Adv. Atmos. Sci.*, **20**, 128-138.

Luo, Y., H. Wang, R. Zhang, W. Qian, and Z. Luo, 2013: Comparison of rainfall characteristics and convective properties of monsoon precipitation systems over South China and the Yangtze and Huai River Basin. *J. Climate*, **26**, 110-132, doi:10.1175/JCLI-D-12-00100.1.

_____, and Coauthors, 2017: The Southern China Monsoon Rainfall Experiment (SCMREX). *Bull. Amer. Meteor. Soc.,* **98**, 999-1013, doi:10.1175/BAMS-D-15-00235.1.

Magagi, R., and A. P. Barros, 2004: Estimation of latent heating of rainfall during the onset of the Indian Monsoon using TRMM PR and Radiosonde data. *J. Appl. Meteorol.*, **43**, 328-349.

McCumber, M., W.-K. Tao, J. Simpson, R. Penc, and S.-T. Soong, 1991: Comparison of ice-phase microphysical parameterization schemes using numerical simulations of tropical convection. *J. Appl. Meteorol.*, **30**, 985-1004.

Mechoso, C. R., and Coauthors, 2013: Ocean-cloud-atmosphere-land interactions in the southeastern Pacific: The VOCALS program. *Bull.Amer. Meteor. Soc.*, **95**, 357-375.

Meng, W.-G., J.-N. Li, A.-Y. Wang, S.-K. Fong, C.-M. Ku, and J.-H. Yan, 2005: Effects of condensation heating and surface fluxes on the development of a south china mesoscale convective system (MCS). *J. Trop. Meteorol.*, **21**, 368-376.

Mlawer, E. J., S. J. Taubman, P. D. Brown, M. J. Iacono, and S. A. Clough, 1997: Radiative transfer for inhomogeneous atmospheres: RRTM, a validated correlated-k model for the longwave. *J. Geophys. Res.*, **102**, 16663-16682.

Niu, G.-Y., and Coauthors, 2011: The community Noah land surface model with multiparameterization options (Noah-MP): 1. Model description and evaluation with local-scale measurements. *J. Geophys. Res.*, **116**, D12109, doi:10.1029/2010JD015139.

Papritz, L., and S. Pfahl, 2015: Importance of latent heating in mesocyclones for the decay of cold air outbreaks: A numerical process study from the Pacific sector of the Southern Ocean. *Mon. Wea. Rev.*, **144**, 315-336, doi:10.1175/MWR-D-15-0268.1.

Pfahl, S., C. Schwierz, M. Croci-Maspoli, C. M. Grams, and H. Wernli, 2015: Importance of latent heat release in ascending air streams for atmospheric blocking. *Nat. Geosci.*, **8**, 610-614, doi:10.1038/ngeo2487.

Qian, J.-H., 2008: Why precipitation is mostly concentrated over islands in the maritime continent. *J. Atmos. Sci.*, **65**, 1428-1441.

Qian, Y., and Y. Shen, 1990: Numerical prediction experiments of effects of diabatic heating process on circulation and weather in the tropical and subtropical regions. *J. Trop. Meteorol.*, **6**, 193-202.

Tao, W.-K., and J. Simpson, 1993: The Goddard cumulus ensemble model. Part I: Model description. *Terr. Atmos. Oceanic Sci.*, **4**, 35-72.

_____, C. L. Shie, J. Simpson, S. Braun, R. H. Johnson, and P. E. Ciesielski, 2003: Convective systems over the South China Sea: Cloud-resolving model simulations. *J. Atmos. Sci.*, **60**, 2929-2956.

_____, D. Wu, T. Matsui, C. Peters-Lidard, S. Lang, A. Hou, M. Rienecker, W. Petersen, and M. Jensen, 2013: Precipitation intensity and variation during MC3E: A numerical modeling study. *J. Geophys. Res.*, **118**, 7199-7218, doi:10.1002/jgrd.50410.

Tao, Y., Y. Qi, and Y. Hong, 2012: Numerical study of the influence of the latent heat on the mesoscale convective system and precipitation during a torrential rain event in North China. *Acta Meteor. Sin.*, **70**, 50-64, doi:10.11676/qxxb2012.005.

Thielen, J., W. Wobrock, A. Gadian, P. G. Mestayer, and J.-D. Creutin, 2000: The possible influence of urban surfaces on rainfall development: a sensitivity study in 2D in the meso-γ-scale. *Atmos. Res.*, **54**, 15-39.

Wang, P., Z. Ruan, and H. W. Kang, 2002: Numerical study on cloud physical processes of heavy rainfall in south China. *J. Appl. Meteorol. Sci.*, **13**, 78-87 (In Chinese with English abstract).

Wang, Y., X. Shen, and X. Li, 2010: Microphysical and radiative effects of ice clouds on responses of rainfall to the large-scale forcing during pre-summer heavy rainfall over southern China. *Atmos. Res.*, **97**, 35-46, doi:10.1016/j.atmosres.2010.03.005.

Wen, L., L. S. Cheng, H. C. Zuo, and S. H. Lue, 2006: Numerical simulation and analysis on the cloud microphysics fields of "98.5" heavy rainfall of south China in pre-summer flood season. *Plateau Meteor.*, **25**, 423-429 (In Chinese with English abstract).

Wu, L., R. Huang, H. He, Y. Shao, and Z. Wen, 2010: Synoptic characteristics of heavy rainfall events in pre-monsoon season in South China. *Adv. Atmos. Sci.*, **27**, 315-327, doi:10.1007/s00376-009-8219-z.

_____, Y. Shao, and A. Y. S. Cheng, 2011: A diagnostic study of two heavy rainfall events in South China. *Meteorol. Atmos. Phys.*, **111**, 13-25, doi:10.1007/s00703-010-0112-x.

Xu, X., X. Yu, J. Dai, G. Liu, Y. Zhu, and Z. Yue, 2011: Direct observation from sounding of the warming caused by homogeneous freezing in a severe storm. *Trans. Atmos. Sci.*, **34**, 416-422, doi:10.13878/j.cnki.dqkxxb.2011.04.007 (In Chinese with English abstract).

Yin, J., 2013: The Study on Observation and Prarmeterization of Cloud-Precipitation Microphysical Properties over East Asia. Doctoral thesis, Zhejiang University, 66-106 (In Chinese with English abstract).

_____, D. Wang, and G. Zhai, 2011: Long-term in situ measurements of the cloud-precipitation microphysical properties over East Asia. *Atmos. Res.*, **102,** 206-217, doi:10.1016/j.atmosres.2011.07.002.

_____, _____, and _____, 2012: An evaluation of ice nuclei characteristics from the long-term measurement data over North China. *Asia-Pac. J. Atmos. Sci.*, **48**, 197-204, doi 10.1007/s13143-012-0020-8.

_____, _____, and _____, 2013a: A comparative study of cloud-precipitation microphysical properties between East Asia and other regions. *J. Meteor. Soc. Japan*, **91**, 507-526, doi:10.2151/jmsj.2013-406.

_____, _____, _____, and Z. Wang, 2013b: Observational characteristics of cloud vertical profiles over the continent of East Asia from the CloudSat data. *Acta Meteor. Sin.*, **27**, 26-39, doi:10.1007/s13351-013-0104-0.

_____, _____, _____, and H.-B. Xu, 2014: An investigation into the relationship between liquid water content and cloud number concentration in the stratiform clouds over north China. *Atmos. Res*., **139**, 137-143, doi:10.1016/j.atmosres.2013.12.004.

_____, _____, and _____, 2015: An attempt to improve Kessler-type parameterization of warm cloud microphysical conversion processes using Cloudsat observations. *J. Meteor. Res*., **29**, 82-92, doi:10.1007/s13351-015-4091-1.

Zängl, G., 2007: Interaction between dynamics and cloud microphysics in orographic precipitation enhancement: A high-resolution modeling study of two north alpine heavy-precipitation events. *Mon. Wea. Rev.*, **135**, 2817-2840.

Zhang, R., Y. Ni, L. Liu, Y. Luo, and Y. Wang, 2011a: South China heavy rainfall experiments (SCHeREX). *J. Meteor. Soc. Japan*, **89**, 153-166, doi:10.2151/jmsj.2011-A10.

Zhang, X.-H., and Y. Ni, 2009: A comparative study of a frontal and a non-frontal convective systems. *Acta Meteor. Sin.*, **67**, 108-121 (in Chinese).

Zhang, X.-M., W. Meng, Y. Zhang, and J. Liang, 2011b: Analysis of mesoscale convective systems associated with a warm-sector rainstorm event over south China. *J. Trop. Meteorol.*, **11**, 1-10, doi:10.3969/j.issn.1006-8775.2011.01.001 (In Chinese with English abstract).

Zhao, S., N. Bei, and J. Sun, 2007: Mesoscale analysis of a heavy rainfall event over Hong Kong during a pre-rainy season in South China. *Adv. Atmos. Sci.*, **24**, 555-572.

Zhao, Y., Z. Li, and Z. Xiao, 2008: Comparison analysis of south China front and warm-area heavy rain systems in June 2006. *Meteor. Sci. Tech.*, **36**, 48-53.

Zhou, X., J. Xue, and Z. Tao, 2003: *Torrential Rainfall Experiment over Both Sides of the Taiwan Strait and Adjacent Area (HUAMEX).* Meteorological Press, 370 pp.